



Gazi University

**Journal of Science**

PART A: ENGINEERING AND INNOVATION

<http://dergipark.org.tr/guj.1393092>

## Comparative Analysis of Optimal Control Strategies: LQR, PID, and Sliding Mode Control for DC Motor Position Performance

Hakan KIZMAZ<sup>1\*</sup> <sup>1</sup> Department of Electrical and Electronics Engineering, Faculty of Engineering and Architecture, Batman University, Batman, Türkiye

Keywords	Abstract
DC Motor Linear Quadratic Regulator Optimal Control Optimal PID Optimal Integral Sliding Mode Control	This study applies these control methods to the DC motor system to examine the robustness and performance of four optimal control methods. Optimal controllers aim to control the system to minimize a selected performance index. These control methods offer advantages such as improving energy efficiency, reducing costs, and enhancing system security. The Linear Quadratic Regulator (LQR) based controller is the primary optimal control method. Two well-known traditional control techniques include the Proportional-Integral-Derivative (PID) and Integral Sliding Mode Controller (ISMC). However, they do not usually contain optimal properties. In this study, the optimal control algorithms, defined by obtaining controller parameters through the Riccati equation, are applied to achieve accurate position-tracking control in a DC motor system using Matlab/Simulink. The integral term-based algorithms seem to be robust and eliminate steady-state errors. The optimal PID controller could not provide the minimum performance index, unlike the other controllers in the study. LQR and optimal ISMC algorithms could allow the performance index to be a minimum. An illustrative comparison of the performances of all optimal control algorithms has been presented through graphical representation, along with corresponding interpretations.

### Cite

Kizmaz, H. (2023). Comparative Analysis of Optimal Control Strategies: LQR, PID, and Sliding Mode Control for DC Motor Position Performance. *GU J Sci, Part A, 10(4)*, 571-592. doi:10.54287/guj.1393092

Author ID (ORCID Number)	Article Process
0000-0001-7680-7191 Hakan KIZMAZ	<b>Submission Date</b> 19.11.2023 <b>Revision Date</b> 13.12.2023 <b>Accepted Date</b> 26.12.2023 <b>Published Date</b> 31.12.2023

## 1. INTRODUCTION

DC motors are extensively utilized in applications involving velocity and position control, especially robotics (He et al, 2023). They actuate components in various electronic projects, including inverted pendulum systems (Mondal & Dey, 2020), self-balancing robots (Feng et al., 2023), and uncrewed vehicles (Tanveer & Ahmad, 2023). DC motors are preferred over their AC counterparts due to their lower power consumption and ease of maintenance. However, achieving precise control over the angular position of a DC motor remains challenging.

Position control of DC motors has been thoroughly investigated in the literature, resulting in well-defined system transfer functions and state space equations. When working with such systems, controllers that utilize the known system model for control law derivation offer significant advantages in design simplicity, hardware implementation, and adaptability. DC motors are favored for their cost-effectiveness, low power consumption, and precision in servo applications. However, the main challenge in controlling systems with DC motors is accurately calculating the necessary electrical power to attain the desired motor angular position or speed.

An optimal control system seeks to maximize system benefit while minimizing costs, involving a viable control strategy within defined constraints to optimize a system's performance. In a controlled dynamic system, the goal is to find the best control plan from a set of permissible plans, enabling the system to transition from its initial state to a desired target state while enhancing system performance. In linear systems, optimal control

\*Corresponding Author, e-mail: [hakan.kizmaz@batman.edu.tr](mailto:hakan.kizmaz@batman.edu.tr)

typically translates into a linear-quadratic problem. This approach is widely acknowledged for systematically designing controllers to optimize performance according to a specified index. In the literature, there are studies in the field of optimal control of DC motors using various artificial neural networks (Khomeenko et al., 2013; Wang et al., 2019) or metaheuristic algorithms (Mamta & Singh, 2020; Rasheed, 2020). However, despite yielding successful results, these algorithms come with a high computational burden.

The (LQR) is a linear optimal controller that harnesses the state space model to derive the control, utilizing state variables of the system for control law formulation. LQR is formulated to minimize both the square of the error and the energy required to attain the same objective concurrently. Solving the algebraic Riccati equation results in the optimal control law, characterized by a steady gain matrix for linear time-invariant systems. After selecting the appropriate weighting matrices in the performance index, the state feedback gain can be tailored to meet specific requirements. However, the robustness of a state feedback control system relying solely on a constant gain matrix cannot be guaranteed. To ensure robustness in LQR control, we employ the integral of the output variable within the control system. This type of control function, known in the literature as LQR with integral action, exhibits robustness against system uncertainties and steady-state errors (Ruderman et al., 2008).

PID controllers are a straightforward and effective way to regulate plants. The PID controller is widely used in control engineering for its simplicity and effectiveness, and it has a rich history in the field. The three controller gain parameters are typically set as constants. Nonetheless, manual fine-tuning of the PID controller demands substantial human intervention, constituting a significant limitation. PID controller parameters are usually determined to achieve the desired system behaviour using pole placement. The desired behaviour of the system can be in terms of settling time for system state variables or optimizing energy consumption within the system. An alternative but more complex approach involves using optimal controllers, which seek the optimal solution by solving the algebraic Riccati equation. These strategies require a linear system and complete state feedback for implementation. However, a system incorporating a PID controller can be transformed into a feedback system where the Riccati equation can be applied through specific mathematical manipulations. Mukhopadhyay (1978) includes such a study.

Sliding mode control (SMC) theory, initially developed for variable structure systems, has since become emblematic of this class of control systems. During its early development, SMC theory was secondary to linear control theory. Recent efforts have refocused on variable structure control strategies using sliding-mode techniques for DC servo drive systems. SMC offers distinct advantages, including robust performance in unmodeled dynamics, insensitivity to parameter variations, and resilience against external disturbances. These benefits find practical application in controlling position and speed in DC servo systems (Durdu & Dursun, 2019; Eli et al., 2023; Saputra, et al., 2023).

The SMC design process consists of two primary stages. Initially, a sliding surface is selected to represent the desired closed-loop performance. Subsequently, a control strategy is formulated to guide the system state trajectory towards this surface. The period before reaching the sliding surface is called the "reaching phase." External disturbances, including matched ones, affect the system during this reaching phase. An Integral Sliding Mode was introduced to eliminate the reaching phase and maintain a sliding mode. ISMC is mainly employed in cases where a steady-state error in the system needs correction. An integrator-term compensator is added to the sliding surface expression to eliminate the steady-state error. Adding a compensator to the SMC system introduces extra dynamics, increasing the system's order compared to the original setup. Typically, performance evaluation involves quadratic functions of state variables and control inputs. Solving the algebraic Riccati equation provides the optimal control law for a linear time-invariant system with a constant gain matrix. Once weighting matrices are chosen, the feedback gain can be customized for specific needs. However, the robustness of the optimal gain may not match that of the pole-placement gain. Integrating LQR design principles into the SMC framework is crucial. This situation is presented in by Utkin (1977).

In Yu et al. (2004), a method that integrates LQR and SMC techniques is proposed for the design of the DC motor position control system. A. Yosef (2011) proposed an integral control-based SMC for DC motor servo control. In Gorczyca et al. (2011) presented a work about optimal control of the linear and the nonlinear DC motor model. The nonlinear optimal control solutions are obtained using the mean square error method.

Marva et al. proposed a controller strategy comprising the optimal control law and integral sliding mode (Jouini et al., 2019). Maghfiroh et al. (2022) improved the LQR control of the DC motor. Their study was about the optimization of the LQR algorithm. Aravind et al. (2017) deal with implementing linear quadratic Gaussian and extended Kalman filters for DC motors. Xiang and Wei (2021) made a work about a DC motor position tracking system based on LQR. Pratama et al. (2022) employed an optimal quadratic regulator PID for DC motor angular velocity control.

In this article, some of the mentioned optimal control algorithms may require a different number of measurable state variables than others. This study has not analyzed the algorithms' need for measurable state variables. Readers searching for a solution in this regard can refer to the topics of observers and estimators in control and system theory. Observers like Luenberger (Davis, 2002) and Kalman (Simon, 2006) are the most used algorithms for estimating unmeasurable state variables.

This study presents a comparative simulation analysis that centres on implementing four distinct optimal control methods for the positional control of a DC motor. Notably, all methods commonly employ the Riccati equation as a fundamental component. Furthermore, these algorithms are formulated to minimize or maximize a designated performance index. The study meticulously explores the impact of these algorithms on the state variables and performance indices of the DC motor model. The findings are effectively illustrated through comparative graphs. This unique methodology serves the purpose of discerning the practical efficacy of these methods in the context of DC motor applications, thus offering a valuable contribution to industrial and automation literature.

This paper is structured in the following manner: The section titled 'Preliminaries and Mathematical Background' provides an overview of a range of optimal control algorithms rooted in the Riccati equation and conventional control methods. The section titled 'DC Servo Machine Mathematical Model' offers an in-depth exposition of the mathematical underpinnings of the DC machine model. The section 'Computational Findings' details the numerical computations associated with the optimal control algorithms. The section on 'Simulation Results' presents the outcomes of the aforementioned optimal control approaches. Finally, the 'Conclusions' section offers a summarization of the paper.

## 2. PRELIMINARIES AND MATHEMATICAL BACKGROUND

This section summarizes the theories and mathematical expressions used in this paper. Consider the following linear system,

$$\dot{\mathbf{x}}(t) = \mathbf{A}\mathbf{x}(t) + \mathbf{B}\mathbf{u}(t) \quad (1)$$

where  $\mathbf{A} \in \mathcal{R}^{n \times n}$  is the state matrix,  $\mathbf{B} \in \mathcal{R}^{n \times r}$  the system input matrix,  $\mathbf{x} \in \mathcal{R}^{n \times 1}$  is the state vector and  $\mathbf{u} \in \mathcal{R}^{r \times 1}$  is system input vector. The indices  $n$  and  $r$  refer to the number of state variables and the number of system inputs, respectively. The output equation of a linear system,

$$\mathbf{y}(t) = \mathbf{C}\mathbf{x}(t) \quad (2)$$

where  $\mathbf{C} \in \mathcal{R}^{m \times n}$  is output matrix. The indices  $m$  is referred to the number of outputs.

The optimal control problem can be calculated as a control input  $\mathbf{u}(t)$  that satisfies the system to follow an optimal state variables trajectory. An initial cost function is established. The control input must minimize the cost function as much as possible.

Dreyfus (1962) offered a method for deriving a series of differential equations that exhibit boundary condition properties, referred to as the Euler-Lagrange equations. The exact boundary conditions can be provided using the Hamiltonian function, employing the Pontryagin (1986) maximum principle.

Hamilton-Jacobi-Bellman (HJB) partial differential equation is one of the main approaches to solving optimal control problems (Kirk, 1998). The optimality problem with linear quadratic performance criterion is generally solved by Hamilton-Jacobi equations. Solutions of the equations take the form of the matrix Riccati equation. When the system is controllable, that equation provides an optimal control law as a linear function of the state vector components.

The most usable quadratic performance index is as follows.

$$J = \int_{t_0}^{t_1} (\mathbf{x}^T \mathbf{Q} \mathbf{x} + \mathbf{u}^T \mathbf{R} \mathbf{u}) dt \quad (3)$$

where  $J$  is a scalar quantity,  $\mathbf{Q} \in \mathcal{R}^{n \times n}$  and  $\mathbf{R} \in \mathcal{R}^{r \times r}$  the state and control weighting matrices, respectively. Besides, they are always symmetric, positively defined, and square. Optimal control problems include crucial performance criteria such as settling time and the consumed energy for system control. These two criteria have the opposite operating mentality. When the weight entries of the  $\mathbf{Q}$  matrix are selected as equal to the weights of the  $\mathbf{R}$  matrix, the system's energy consumption has equal importance with the settling time. When the  $\mathbf{Q}$  matrix weights are selected bigger than the  $\mathbf{R}$  matrix weights, the settling time is more important than energy consumption. Namely, to reduce the settling time, the energy consumption is ignored. When the  $\mathbf{Q}$  matrix weights are selected less than the  $\mathbf{R}$  matrix weights, the energy consumption is as low as possible.

## 2.1. Linear Quadratic State Feedback Controller

Upon consideration of Eq. (1) and (3), application of the Hamiltonian theorem to these equations yields the following expression (Kirk, 1998; Burns, 2001),

$$\mathbf{u}_{lqr} = -\mathbf{K}_{lqr} \mathbf{x} = -\mathbf{R}^{-1} \mathbf{B}^T \mathbf{P}_{lqr} \mathbf{x} \quad (4)$$

where  $\mathbf{u}_{lqr}$  is the optimal control input,  $\mathbf{P}_{lqr} \in \mathcal{R}^{n \times n}$  is a square symmetric adjoint matrix,  $\mathbf{P}_{lqr}(t)$  are found by Eq. (5).

$$\dot{\mathbf{P}}_{lqr} = -\mathbf{P}_{lqr} \mathbf{A} - \mathbf{A}^T \mathbf{P}_{lqr} - \mathbf{Q}_{lqr} + \mathbf{P}_{lqr} \mathbf{B} \mathbf{R}^{-1} \mathbf{B}^T \mathbf{P}_{lqr} \quad (5)$$

As time integration in a backward direction advance, Kalman demonstrated that  $\mathbf{P}_{lqr}(t)$  solutions stabilize at constant values. In that case, Eq. (5),

$$0 = -\mathbf{P}_{lqr} \mathbf{A} - \mathbf{A}^T \mathbf{P}_{lqr} - \mathbf{Q}_{lqr} + \mathbf{P}_{lqr} \mathbf{B} \mathbf{R}^{-1} \mathbf{B}^T \mathbf{P}_{lqr} \quad (6)$$

Eq. (5)-(6) are continuous solutions of the matrix Riccati equation. Solving Eq. (6) yields the  $\mathbf{P}_{lqr}$  matrix. Substituting the  $\mathbf{P}_{lqr}$  matrix into Eq. (4) concluded optimal control input with feedback matrix  $\mathbf{K}_{lqr}$ . The linear feedback control system is considered in Figure 1. When the matrix  $\mathbf{K}_{lqr}$  is substituted into Figure 1, the control system becomes a linear quadratic feedback control system or LQR (Burns, 2001). Attention should be drawn to the existence of state feedback in Figure 1. It should be noted that the state feedback algorithms may need to possess observable state variables or use an observer for such situations.

It is commonly assumed that LQRs, as depicted in Figure 1, are primarily used for scenarios where the set point is equal to zero. However, the set point regulation requires driving the system states to the desired set point state vector  $\mathbf{x}_d$  from any initial state and under disturbance. The set point regulation is generally proposed in industrial applications. This paper aims to use the linear quadratic techniques for set point regulation processes. As a first step, the calculation of the desired control input,  $\mathbf{u}_d$ , that needs to be applied to obtain the desired state vector is required. The derivative terms within Eq. (1) are equated to zero, resulting in the calculation of the control input,  $\mathbf{u}_d$ , corresponding to the obtained  $\mathbf{x}_d$  vector is derived.

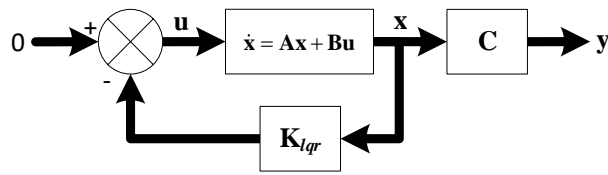


Figure 1. LQR block diagram

$$0 = \mathbf{A}\mathbf{x}_d + \mathbf{B}\mathbf{u}_d \quad (7)$$

where  $\mathbf{x}_d$  is a constant steady-state vector, also called system equilibrium point. Considering matrix  $\mathbf{B}$  has full rank, the desired control input,  $\mathbf{u}_d$ , is determined as,

$$\mathbf{u}_d = -(\mathbf{B}^T \mathbf{B})^{-1} \mathbf{B}^T \mathbf{A} \mathbf{x}_d \quad (8)$$

The desired state vector,  $\mathbf{x}_d$ , might be feasible by directly applying the control input,  $\mathbf{u}_d$ , to the open-loop system. However, open-loop applications would not ensure slight overshoot or robustness against disturbances. Utilizing a feedback control algorithm is a dependable approach to improve system transient behaviour and reject disturbances. The control algorithm necessitates the determination of the system's error dynamics as follows,

$$\left. \begin{aligned} \tilde{\mathbf{x}} &= \mathbf{x} - \mathbf{x}_d, \Rightarrow \mathbf{x} = \tilde{\mathbf{x}} + \mathbf{x}_d \\ \tilde{\mathbf{u}} &= \mathbf{u} - \mathbf{u}_d, \Rightarrow \mathbf{u} = \tilde{\mathbf{u}} + \mathbf{u}_d \end{aligned} \right\} \quad (9)$$

Differentiating state error expression in Eq. (9) and substituting in (1) provides the following,

$$\dot{\mathbf{x}} = \dot{\tilde{\mathbf{x}}} + \dot{\mathbf{x}}_d = \mathbf{A}(\tilde{\mathbf{x}} + \mathbf{x}_d) + \mathbf{B}(\tilde{\mathbf{u}} + \mathbf{u}_d) \quad (10)$$

Here,  $\mathbf{x}_d$  is the equilibrium point and contains constant entries. Since the derivative of a constant is zero, by substituting  $\dot{\mathbf{x}}_d = 0$  and Eq. (7) into Eq. (10), the following expression is derived,

$$\dot{\tilde{\mathbf{x}}} = \mathbf{A}\tilde{\mathbf{x}} + \mathbf{B}\tilde{\mathbf{u}} \quad (11)$$

Eq. (11) defines the error dynamics and allows for direct application of an LQR algorithm.

$$J_{lqr} = \int_{t_0}^{t_1} (\tilde{\mathbf{x}}^T \mathbf{Q} \tilde{\mathbf{x}} + \tilde{\mathbf{u}}^T \mathbf{R} \tilde{\mathbf{u}}) dt \quad (12)$$

The following form of the feedback control optimizes the cost function Eq. (12)

$$\tilde{\mathbf{u}} = -\mathbf{K}_{lqr} \tilde{\mathbf{x}} \quad (13)$$

where the matrix  $\mathbf{K}_{lqr}$  is defined by

$$\mathbf{K}_{lqr} = \mathbf{R}^{-1} \mathbf{B}^T \mathbf{P} \quad (14)$$

Incorporating Eq. (13) into Eq. (11), the closed-loop system equation is obtained as follows,

$$\dot{\tilde{\mathbf{x}}} = (\mathbf{A} - \mathbf{B}\mathbf{K}_{lqr}) \tilde{\mathbf{x}} \quad (15)$$

The eigenvalues of  $\mathbf{A} - \mathbf{BK}_{lqr}$  are placed in the left half of the complex s-plane. That proves the system is asymptotically stable and provides a steady state. In the steady state, the system state  $\mathbf{x}$  becomes  $\mathbf{x}_d$ . Substituting Eq. (9) into Eq. (15) yields the following equation,

$$\dot{\mathbf{x}} = (\mathbf{A} - \mathbf{BK}_{lqr})\mathbf{x} - (\mathbf{A} - \mathbf{BK}_{lqr})\mathbf{x}_d \quad (16)$$

The error variables Eq. (8)-(9) and the feedback control Eq. (13) satisfy the following equation.

$$\mathbf{u} = -[(\mathbf{B}^T\mathbf{B})^{-1}\mathbf{B}^T - \mathbf{K}_{lqr}] \mathbf{x}_d - \mathbf{K}_{lqr}\mathbf{x} \quad (17)$$

In summary, the equilibrium point at the set point is calculated first. Then, the processes defined by Eq. (6),(8), and Eq. (14) are executed, respectively. Finally, optimal control input Eq. (17) is obtained. The entire algorithm is executed as depicted in Figure 2 (Naidu, 2002; Anderson & Moore, 2007).

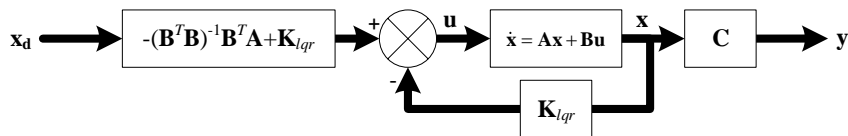


Figure 2. LQR tracking control block diagram

## 2.2. LQR With Integral Control Action (LQRI)

Control algorithms aim to achieve stability, the desired transient response, and minimize steady-state error. The LQR algorithm may not eliminate steady-state error if there are no closed-loop system poles at the origin of the complex plane. The same situation arises when the DC gain of the closed-loop system with a state feedback controller differs from unity.

Steady-state error elimination decreases the disparity between the system's input and output. This action is provided by adding an integral term of the open-loop system. This section discusses using integral terms with a linear quadratic feedback controller (Dorf & Bishop, 2010; Ogata, 2010).

The basic mentality here is to enlarge the original closed-loop system with a linear quadratic controller. Substituting Eq. (4) into Eq. (1) concluded the following equation.

$$\dot{\mathbf{x}} = (\mathbf{A} - \mathbf{BK}_{lqr})\mathbf{x} \quad (18)$$

Eq. (18) is stable when the eigenvalues of  $\mathbf{A} - \mathbf{BK}_{lqr}$  expression are at the left half complex plane. Linear quadratic state feedback controller enables stabilization. However, comprehensive control of steady-state error is achieved by implementing the following procedures.

The integration of error between output and reference input,  $\mathbf{x}_i$ , is as follows,

$$\mathbf{x}_i = \int (\mathbf{r} - \mathbf{y})dt = \int (\mathbf{r} - \mathbf{C}\mathbf{x})dt \quad (19)$$

where the reference control input vector of the system is  $\mathbf{r}$ , the integration error is taken as a new state variable. The derivative of Eq. (19) is as follows,

$$\dot{\mathbf{x}}_i = \mathbf{r} - \mathbf{C}\mathbf{x} \quad (20)$$

By combining Eq. (20) with the original system equations (1) and (2), the augmented state space system is obtained as follows.

$$\begin{aligned} \begin{bmatrix} \dot{\mathbf{x}} \\ \dot{\mathbf{x}}_i \end{bmatrix} &= \begin{bmatrix} \mathbf{A} & 0_{n \times m} \\ -\mathbf{C} & 0_{m \times m} \end{bmatrix} \begin{bmatrix} \mathbf{x} \\ \mathbf{x}_i \end{bmatrix} + \begin{bmatrix} \mathbf{B} \\ 0_{m \times r} \end{bmatrix} \mathbf{u} + \begin{bmatrix} 0_{n \times m} \\ \mathbf{I}_{m \times m} \end{bmatrix} \mathbf{r} \\ \mathbf{y} &= [\mathbf{C} \quad 0_{m \times m}] \begin{bmatrix} \mathbf{x} \\ \mathbf{x}_i \end{bmatrix} \end{aligned} \quad (21)$$

$\mathbf{I}_{m \times m}$  is the  $m \times m$  dimensional identity matrix. Eq. (21) includes a new state space vector. In this situation, the state-feedback controller has the following form.

$$\mathbf{u} = -\underbrace{[\mathbf{K}_x \quad \mathbf{K}_{in}]}_{\mathbf{K}_{lqri}} \begin{bmatrix} \mathbf{x} \\ \mathbf{x}_i \end{bmatrix} = -\mathbf{K}_x \mathbf{x} - \mathbf{K}_{in} \mathbf{x}_i \quad (22)$$

the  $\mathbf{K}_x \in \mathfrak{R}^{r \times n}$  is the original state feedback control matrix, and  $\mathbf{K}_{in} \in \mathfrak{R}^{r \times m}$  is the integral control feedback matrix.  $\mathbf{K}_x$  and  $\mathbf{K}_{in}$  form the matrix  $\mathbf{K}_{lqri} \in \mathfrak{R}^{r \times (m+n)}$ . The extended system matrices are as in Eq. (23).

$$\mathbf{x}_{lqri} = \begin{bmatrix} \dot{\mathbf{x}} \\ \dot{\mathbf{x}}_i \end{bmatrix}, \mathbf{A}_{lqri} = \begin{bmatrix} \mathbf{A} & 0_{n \times m} \\ -\mathbf{C} & 0_{m \times m} \end{bmatrix}, \mathbf{B}_{lqri} = \begin{bmatrix} \mathbf{B} \\ 0_{m \times r} \end{bmatrix}, \mathbf{C}_{lqri} = [\mathbf{C} \quad 0_{m \times m}], \mathbf{B}_r = \begin{bmatrix} 0_{n \times m} \\ \mathbf{I}_{m \times m} \end{bmatrix} \quad (23)$$

Substituting Eq. (22) into Eq. (21) yields

$$\dot{\mathbf{x}}_{lqri} = (\mathbf{A}_{lqri} - \mathbf{B}_{lqri} \mathbf{K}_{lqri}) \mathbf{x}_{lqri} + \mathbf{B}_r \mathbf{r} \quad (24)$$

The eigenvalues of  $\mathbf{A}_{lqri} - \mathbf{B}_{lqri} \mathbf{K}_{lqri}$  are placed in the left half of the complex  $s$  plane for asymptotically stable. The cost function related to the augmented state-space system is defined as follows.

$$J_{lqri} = \int_{t_0}^{t_1} (\mathbf{x}_{lqri}^T \mathbf{Q}_{lqri} \mathbf{x}_{lqri} + \mathbf{u}^T \mathbf{R} \mathbf{u}) dt \quad (25)$$

The matrices are substituted in Eq. (26), and the extended costate  $\mathbf{P}_{lqri}$  matrix is calculated.

$$0 = -\mathbf{P}_{lqri} \mathbf{A}_{lqri} - (\mathbf{A}_{lqri})^T \mathbf{P}_{lqri} - \mathbf{Q}_{lqri} + \mathbf{P}_{lqri} \mathbf{B}_{lqri} (\mathbf{R})^{-1} (\mathbf{B}_{lqri})^T \mathbf{P}_{lqri} \quad (26)$$

$\mathbf{Q}_{lqri}$  extended state weight matrix,  $\mathbf{P}_{lqri}$  matrix is used in Eq. (27), and feedback control matrix  $\mathbf{K}_{lqri}$  is obtained.

$$\mathbf{K}_{lqri} = [\mathbf{K}_x \quad \mathbf{K}_{in}] = \mathbf{R}^{-1} \mathbf{B}_{lqri}^T \mathbf{P}_{lqri} \quad (27)$$

$\mathbf{R}$  and  $\mathbf{B}_{lqri}$  matrices are extended control weight and system input matrices.

All obtained matrices  $\mathbf{K}_x$  and  $\mathbf{K}_{in}$  are replaced in Figure 3, and the control system is executed (Ogata, 2010; Nise, 2011).

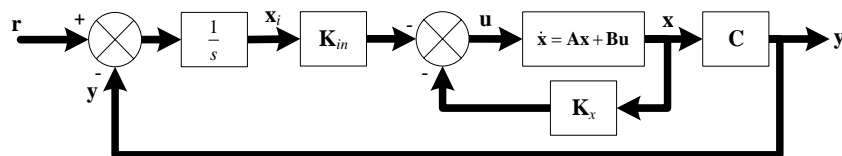


Figure 3. LQR with integral action

### 2.3. Optimal PID Controller

The algorithms given under the subheadings so far use state variables. This case necessitates observable state variables. The state observers are employed for this purpose. Luenberger observer, reduced order observer, or

Kalman estimator can be employed to estimate any observed state variables of any system (Davis, 2002; Simon, 2006).

However, the PID controller may not need any observer since it is an output-based controller, as seen in Figure 4. The feedback is implemented from output to input. The PID controller requires a smaller number of measurable outputs ( $y$ ) of the system. The input signal  $u$  is a three-term controller as follows (Paraskevopoulos, 2002; Franklin et al., 2009; Ogata, 2010):

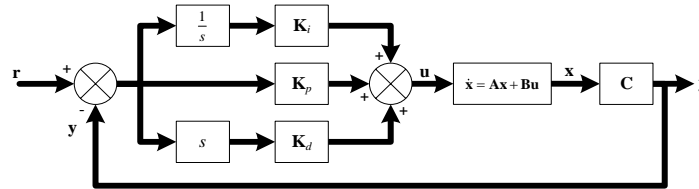


Figure 4. PID control system

$$\mathbf{u} = -\mathbf{K}_p(\mathbf{r} - \mathbf{y}) - \mathbf{K}_i \int_0^t (\mathbf{r} - \mathbf{y})dt - \mathbf{K}_d(\dot{\mathbf{r}} - \dot{\mathbf{y}}) \quad (28)$$

where  $\mathbf{K}_p \in \mathfrak{R}^{m \times r}$ ,  $\mathbf{K}_i \in \mathfrak{R}^{m \times r}$  and  $\mathbf{K}_d \in \mathfrak{R}^{m \times r}$  are proportional, integral, and derivative feedback gain matrices. Considering the help of Eq. (1)-(2) and Eq. (28), Eq. (29) is obtained (Mukhopadhyay, 1978; Pratama, et al., 2022)

$$\begin{aligned} \mathbf{u} &= \left( \mathbf{K}_p \mathbf{r} + \mathbf{K}_i \int \mathbf{r} dt + \mathbf{K}_d \dot{\mathbf{r}} \right) - \mathbf{K}_p \mathbf{C} \mathbf{x} - \mathbf{K}_i \int \mathbf{y} dt - \mathbf{K}_d \mathbf{C} (\mathbf{A} \mathbf{x} + \mathbf{B} \mathbf{u}) \\ &= \mathbf{u}_r - \bar{\mathbf{K}}_p \mathbf{x} - \bar{\mathbf{K}}_i \int_0^t \mathbf{y} dt \end{aligned} \quad (29)$$

Here the gains  $\bar{\mathbf{K}}_p$ ,  $\bar{\mathbf{K}}_i$  and the input residue  $\mathbf{u}_r$  are all defined as

$$\bar{\mathbf{K}}_p = (\mathbf{I}_m + \mathbf{K}_d \mathbf{C} \mathbf{B})^{-1} (\mathbf{K}_p \mathbf{C} + \mathbf{K}_d \mathbf{C} \mathbf{A}) \quad (30)$$

$$\bar{\mathbf{K}}_i = (\mathbf{I}_m + \mathbf{K}_d \mathbf{C} \mathbf{B})^{-1} \mathbf{K}_i \quad (31)$$

$$\mathbf{u}_r = \left( \mathbf{K}_p \mathbf{r} + \mathbf{K}_i \int \mathbf{r} dt + \mathbf{K}_d \dot{\mathbf{r}} \right) \quad (32)$$

Eq. (29) demonstrates that the output feedback with the PID controller resembles any state feedback controller. However, the integral term  $\int \mathbf{y} dt$  appears as a new state variable in Eq. (29). The new state variable is then defined as follows.

$$\mathbf{x}_{new} = \int_0^t \mathbf{y} dt \quad (33)$$

The variable then

$$\dot{\mathbf{x}}_{new} = \mathbf{y} = \mathbf{C} \mathbf{x} \quad (34)$$

The augmented state vector of the system is defined as

$$\bar{\mathbf{x}} = \begin{bmatrix} \mathbf{x} \\ \mathbf{x}_{new} \end{bmatrix} \quad (35)$$

The augmented system may now be described as

$$\dot{\bar{\mathbf{x}}} = \bar{\mathbf{A}}\bar{\mathbf{x}} + \bar{\mathbf{B}}\mathbf{u} \quad (36)$$

The augmented system matrix  $\bar{\mathbf{A}}$  and  $\bar{\mathbf{B}}$  are described by

$$\bar{\mathbf{A}} = \begin{bmatrix} \mathbf{A} & 0_{n \times m} \\ \mathbf{C} & 0_{m \times m} \end{bmatrix}, \bar{\mathbf{B}} = \begin{bmatrix} \mathbf{B} \\ 0_{m \times r} \end{bmatrix} \quad (37)$$

The substituting Eq. (35) into the control input Eq. (29) is then,

$$\mathbf{u} = \mathbf{u}_r - \mathbf{K}_{pid}\bar{\mathbf{x}} \quad (38)$$

where  $\mathbf{K}_{pid} = [\bar{\mathbf{K}}_p \quad \bar{\mathbf{K}}_i]$ . Substituting the Eq. (42) into (36) gives

$$\dot{\bar{\mathbf{x}}} = (\bar{\mathbf{A}} - \bar{\mathbf{B}}\mathbf{K}_{pid})\bar{\mathbf{x}} + \bar{\mathbf{B}}\mathbf{u}_r \quad (39)$$

The eigenvalues of  $\bar{\mathbf{A}} - \bar{\mathbf{B}}\mathbf{K}_{pid}$  are placed in the left half of the complex s-plane for asymptotically stable. The performance index of the form given by Eq. (36)

$$J_{pid} = \int_{t_0}^{t_1} (\bar{\mathbf{x}}^T \bar{\mathbf{Q}} \bar{\mathbf{x}} + \mathbf{u}^T \mathbf{R} \mathbf{u}) dt \quad (40)$$

the desired optimal control

$$\mathbf{u}^* = -\mathbf{R}^{-1} \bar{\mathbf{B}}^T \bar{\mathbf{P}} \bar{\mathbf{x}} \quad (41)$$

where the matrix  $\bar{\mathbf{P}}$  is defined as

$$\bar{\mathbf{P}}\bar{\mathbf{A}} + \bar{\mathbf{A}}^T \bar{\mathbf{P}} - \bar{\mathbf{P}}\bar{\mathbf{B}}\mathbf{R}^{-1} \bar{\mathbf{B}}^T \bar{\mathbf{P}} + \bar{\mathbf{Q}} = 0 \quad (42)$$

where  $\bar{\mathbf{Q}} \in \mathfrak{R}^{(n+m) \times (n+m)}$  extended state weight matrix. Comparing the Eq. (29) and Eq. (41) concluded

$$[\bar{\mathbf{K}}_p \quad \bar{\mathbf{K}}_i] = \mathbf{R}^{-1} \bar{\mathbf{B}}^T \bar{\mathbf{P}} \quad (43)$$

where  $\bar{\mathbf{K}}_p \in \mathfrak{R}^{r \times n}$  and  $\bar{\mathbf{K}}_i \in \mathfrak{R}^{r \times m}$ . Once Eq. (43) is obtained, the controller coefficients are all calculated as following expressions

$$[\mathbf{K}_p \quad \mathbf{K}_d] = \bar{\mathbf{K}}_p \bar{\mathbf{C}}^T (\bar{\mathbf{C}} \bar{\mathbf{C}}^T)^{-1} \quad (44)$$

where  $\bar{\mathbf{C}} = [\mathbf{C}^T \quad (\mathbf{C}\mathbf{A} - \mathbf{C}\mathbf{B}\bar{\mathbf{K}}_p)^T]^T$  and

$$\mathbf{K}_i = (\mathbf{I}_m + \mathbf{K}_d \mathbf{C}\mathbf{B}) \bar{\mathbf{K}}_i \quad (45)$$

The last two equations conclude optimal PID controller parameters.

## 2.4. Controller with Optimal Sliding Mode

In this section, it will be demonstrated only how to provide optimality to the sliding mode controller. Variable structure system control theory is a relatively comprehensive subject. The most pioneer works on this subject belong to Utkin (1977, 1992, 1993) and Utkin and Parnakh (1978).

SMC involves bringing the instantaneous states of the system onto the sliding or switching surface created from state variables and keeping them there. The integrated error dynamics should be considered by appending them to the error variable vector. ISMC's subject is concerned with the robustness of the SMC. Readers are referred to Utkin et al. (2009) for details. The augmented error dynamic vector is as follows.

$$\tilde{\mathbf{x}}_{ismc} = \begin{bmatrix} \tilde{\mathbf{x}} \\ \int \tilde{\mathbf{x}} dt \end{bmatrix} \quad (46)$$

The error dynamics equation then becomes as follows by combining integrated error,  $\int \tilde{\mathbf{x}} dt$ , and Eq. (11).

$$\underbrace{\frac{d}{dt} \begin{bmatrix} \tilde{\mathbf{x}} \\ \int \tilde{\mathbf{x}} dt \end{bmatrix}}_{\dot{\tilde{\mathbf{x}}}_{ismc}} = \underbrace{\begin{bmatrix} \mathbf{A} & 0_{n \times n} \\ \mathbf{I}_{n \times n} & 0_{n \times n} \end{bmatrix}}_{\mathbf{A}_{ismc}} \underbrace{\begin{bmatrix} \tilde{\mathbf{x}} \\ \int \tilde{\mathbf{x}} dt \end{bmatrix}}_{\tilde{\mathbf{x}}_{ismc}} + \underbrace{\begin{bmatrix} \mathbf{B} \\ 0_{n \times r} \end{bmatrix}}_{\mathbf{B}_{ismc}} \tilde{\mathbf{u}} \quad (47)$$

The regular form is the most canonic form used for SMC for linear systems. Consider the nominal linear model error dynamic and their integrated variables are given by Eq. (47).  $(\mathbf{A}_{ismc}, \mathbf{B}_{ismc})$  is a controllable pair and  $\text{rank}(\mathbf{B}_{ismc}) = \eta$ . The sliding surface function

$$s(t) = \boldsymbol{\sigma} \tilde{\mathbf{x}}_{ismc}(t) \quad (48)$$

where  $\boldsymbol{\sigma} \in \mathfrak{R}^{\eta \times 2n}$  is the sliding surface coefficient vector and  $s(t)$  is a scalar function.

The dynamic equation of the linear system, defined by Eq. (1)-(2), may be separated into subsystems; only one includes a control signal. A non-singular transformation is used with an orthogonal matrix  $\mathbf{T}$ , to transform the system into the regular form,

$$\mathbf{z}(t) = \mathbf{T} \tilde{\mathbf{x}}_{ismc}(t) \quad (49)$$

Taking derivatives of Eq. (49) and substituting into (47), the following regular form obtained

$$\dot{\mathbf{z}}_1(t) = \mathbf{A}_{11} \mathbf{z}_1(t) + \mathbf{A}_{12} \mathbf{z}_2(t) \quad (50)$$

$$\dot{\mathbf{z}}_2(t) = \mathbf{A}_{21} \mathbf{z}_1(t) + \mathbf{A}_{22} \mathbf{z}_2(t) + \mathbf{B}_2 \mathbf{u}(t) \quad (51)$$

where  $\mathbf{A}_{11} \in \mathfrak{R}^{(2n-\eta) \times (2n-\eta)}$ ,  $\mathbf{A}_{12} \in \mathfrak{R}^{(2n-\eta) \times \eta}$  and  $\mathbf{A}_{21} \in \mathfrak{R}^{\eta \times (2n-\eta)}$ ,  $\mathbf{A}_{22} \in \mathfrak{R}^{\eta \times \eta}$  are all sub-block matrices of transformed  $\mathbf{A}$  matrix.  $\mathbf{B}_2$  is  $\eta$  dimensional matrix.  $\mathbf{z}_1 \in \mathfrak{R}^{(2n-\eta) \times 1}$  and  $\mathbf{z}_2 \in \mathfrak{R}^{\eta \times 1}$  are sub-block vectors. This method is called the decoupling principle as well. The matrix sub-blocks in Eq. (50)-(51),

$$\mathbf{T} \mathbf{A}_{ismc} \mathbf{T}^T = \begin{bmatrix} \mathbf{A}_{11} & \mathbf{A}_{12} \\ \mathbf{A}_{21} & \mathbf{A}_{22} \end{bmatrix}, \quad \mathbf{T} \mathbf{B}_{ismc} = \begin{bmatrix} 0 \\ \mathbf{B}_2 \end{bmatrix} \quad (52)$$

Transformation matrix  $\mathbf{T}$  is an orthogonal matrix and can be calculated by QR decomposition (Golub & Loan, 2013). This is useful to get the decomposition of the input matrix. The sliding surface is written as

$$s(t) = \underbrace{\sigma \mathbf{T}^T}_{\mathbf{S}} \mathbf{z} = \mathbf{S} \mathbf{z} = [\mathbf{S}_1 \quad \mathbf{S}_2] \begin{bmatrix} \mathbf{z}_1 \\ \mathbf{z}_2 \end{bmatrix} = \mathbf{S}_1 \mathbf{z}_1(t) + \mathbf{S}_2 \mathbf{z}_2(t) \quad (53)$$

where the  $\mathbf{S}_1 \in \mathbb{R}^{\eta \times (2n-\eta)}$  and  $\mathbf{S}_2 \in \mathbb{R}^{\eta \times \eta}$  sub-vector of  $\mathbf{S}$ .

The switching function  $s(t)$  equals zero during the sliding motion. Eq. (53) is then equal to zero.

$$\mathbf{S}_1 \mathbf{z}_1(t) + \mathbf{S}_2 \mathbf{z}_2(t) = 0 \quad (54)$$

The variable  $\mathbf{z}_2$  is left alone,

$$\mathbf{z}_2 = -\mathbf{S}_2^{-1} \mathbf{S}_1 \mathbf{z}_1 \quad (55)$$

Eq. (55) is substituted into the Eq. (50) yields,

$$\dot{\mathbf{z}}_1 = [\mathbf{A}_{11} - \mathbf{A}_{12} \mathbf{S}_2^{-1} \mathbf{S}_1] \mathbf{z}_1 \quad (56)$$

To provide asymptotically stability of the system given by Eq. (56), the eigenvalues of  $[\mathbf{A}_{11} - \mathbf{A}_{12} \mathbf{S}_2^{-1} \mathbf{S}_1]$  partition must be at the left-half  $s$ -plane. The unknown partition  $\mathbf{S}_2^{-1} \mathbf{S}_1$  can be calculated by employing the pole placement or optimal control methods.  $\mathbf{S}_2$  may be chosen as a non-singular matrix and calculated according to  $\mathbf{S}_1$ . The equation below will be employed for the calculation of  $\sigma$  vector

$$s(t) = \mathbf{S} \mathbf{z} = \underbrace{\mathbf{S} \mathbf{T}}_{\sigma} \tilde{\mathbf{x}}_{ismc} = \sigma \tilde{\mathbf{x}}_{ismc} \quad (57)$$

When the state variables are not on the sliding surface, there is a need for a reaching rule to drive the state variables onto the sliding surface. In Gao and Hung (1993) proposed a reaching law called a constant plus proportional rate.

$$\dot{s}(t) = -\rho \cdot \text{sign}(s(t)) - k \cdot s \quad (58)$$

where  $\rho > 0$  and  $k > 0$ . The constant parameter  $k$  within the signum function balances the convergence rate during the reaching phase and the magnitude of oscillations experienced during the sliding phase. The introduction of the proportional component enhances convergence rates for larger sliding variable values, allowing for a reduction in the coefficient  $\rho$  without compromising the favorable aspects during the reaching mode. Conversely, as the sliding surface is approached, the impact of the proportional term diminishes, effectively mitigating the potential for increased oscillations during the sliding phase.

Eq. (58) will equal zero, while the state variables are on the sliding surface. Eq. (47) is substituted into the derivative of Eq. (57). The resulting outcome is equated with Eq. (58). The control input  $\mathbf{u}_{ismc}$  is then left alone by considering  $\tilde{\mathbf{u}} = \mathbf{u}_{ismc} - \mathbf{u}_d$ , and the SMC input rule is obtained as follows.

$$\mathbf{u}_{ismc} = \mathbf{u}_d - (\sigma \mathbf{B}_{ismc})^{-1} [\sigma (k\mathbf{I} + \mathbf{A}_{ismc}) \tilde{\mathbf{x}}_{ismc} + \rho \cdot \text{sign}(s)] \quad (59)$$

where  $\mathbf{u}_d$  is defined by Eq. (8).

This subsection discusses the calculation of the  $\mathbf{S}$  vector according to the minimizing cost function criterion. Utkin and Yang (1978) proposed this method as quadratic minimization. It is possible to reach the details (Utkin, 1992; Edwards & Spurgeon, 1998).

SMC action includes two modes: the first is to bring state variable values onto the switching surface. The second mode is to keep all state variables at the sliding surface. Once the second mode is satisfied, the sliding surface equation equals zero. Sliding mode motion does not depend on control input and is defined by the equation of sliding surface. Eq. (3) is not suited to the sliding motion optimality criterion. Control-independent the functional optimality criterion,

$$J_{ismc} = \int_{t_0}^{t_1} (\tilde{\mathbf{x}}_{ismc})^T \mathbf{Q}_{ismc} \tilde{\mathbf{x}}_{ismc} dt \quad (60)$$

It is presumed that the system's state at time  $t_0$ ,  $\mathbf{x}(t_0)$  is a known initial condition and is such that  $\mathbf{x}(t) \rightarrow 0$  as  $t \rightarrow \infty$ . It is needed to be determined that the optimal  $m$ -dimensional control system Eq. (50)-(51) with vector  $\mathbf{z}_2 = (\mathbf{S}_2)^{-1} \mathbf{S}_1 \mathbf{z}_1$  as control and criterion (60) is represented according to (49) transformation.

$$\mathbf{T} \mathbf{Q}_{ismc} \mathbf{T}^T = \begin{bmatrix} \mathbf{Q}_{11} & \mathbf{Q}_{12} \\ \mathbf{Q}_{21} & \mathbf{Q}_{22} \end{bmatrix}, \quad \mathbf{Q}_{21} = \mathbf{Q}_{12}^T \quad (61)$$

The optimality criterion (60) may then be expressed regarding the  $\mathbf{T}$  transformation.

$$J_{ismc} = \int_{t_0}^{t_1} (\mathbf{z}_1^T \mathbf{Q}_{11} \mathbf{z}_1 + 2\mathbf{z}_1^T \mathbf{Q}_{12} \mathbf{z}_2 + \mathbf{z}_2^T \mathbf{Q}_{22} \mathbf{z}_2) dt \quad (62)$$

It is required to reform Eq. (62) in the standard LQR problem as Eq. (3). Thus, it is necessary to eliminate the cross term  $2(\mathbf{z}_1)^T \mathbf{Q}_{12} \mathbf{z}_2$ . The last two in Eq. (62) may be regarded as yield.

$$2\mathbf{z}_1^T \mathbf{Q}_{12} \mathbf{z}_2 + \mathbf{z}_2^T \mathbf{Q}_{22} \mathbf{z}_2 = (\mathbf{z}_2 + \mathbf{Q}_{22}^{-1} \mathbf{Q}_{21} \mathbf{z}_1)^T \mathbf{Q}_{22} (\mathbf{z}_2 + \mathbf{Q}_{22}^{-1} \mathbf{Q}_{21} \mathbf{z}_1) - \mathbf{z}_1^T \mathbf{Q}_{21}^T \mathbf{Q}_{22}^{-1} \mathbf{Q}_{21} \mathbf{z}_1 \quad (63)$$

It is forthright to authenticate that Eq. (62) can be reformed as

$$J_{ismc} = \int_{t_s}^{\infty} (\mathbf{z}_1^T (\mathbf{Q}_{11} - \mathbf{Q}_{12} \mathbf{Q}_{22}^{-1} \mathbf{Q}_{21}) \mathbf{z}_1 + (\mathbf{z}_2 + \mathbf{Q}_{22}^{-1} \mathbf{Q}_{21} \mathbf{z}_1)^T \mathbf{Q}_{22} (\mathbf{z}_2 + \mathbf{Q}_{22}^{-1} \mathbf{Q}_{21} \mathbf{z}_1)) dt \quad (64)$$

Define

$$\hat{\mathbf{Q}} = \mathbf{Q}_{11} - \mathbf{Q}_{12} \mathbf{Q}_{22}^{-1} \mathbf{Q}_{21} \quad (65)$$

$$\mathbf{v} = \mathbf{z}_2 + \mathbf{Q}_{22}^{-1} \mathbf{Q}_{21} \mathbf{z}_1 \quad (66)$$

Eq. (64) can then be written as

$$J_{ismc} = \int_{t_s}^{\infty} (\mathbf{z}_1^T \hat{\mathbf{Q}} \mathbf{z}_1 + \mathbf{v}^T \mathbf{Q}_{22} \mathbf{v}) \quad (67)$$

Recall the original transformed Eq. (50). Taking  $\mathbf{z}_2$  alone in Eq. (66) and substituting it into Eq. (50),

$$\dot{\mathbf{z}}_1 = (\mathbf{A}_{11} - \mathbf{A}_{12} \mathbf{Q}_{22}^{-1} \mathbf{Q}_{21}) \mathbf{z}_1 + \mathbf{A}_{12} \mathbf{v} \quad (68)$$

Hence, the problem turns into minimizing the Eq. (67) subject to the system (68). The problem also can be interpreted as a standard LQR problem. The positive definiteness of  $\mathbf{Q}_{ismc}$  ensures that  $\mathbf{Q}_{22} > 0$  so that the pair  $(\mathbf{A}_{ismc}, \mathbf{B}_{ismc})$  is controllable. Thus, matrix  $\mathbf{P}_{ismc}$  being the unique solution to the matrix Riccati equation,

$$\mathbf{P}_{ismc} (\mathbf{A}_{11} - \mathbf{A}_{12} \mathbf{Q}_{22}^{-1} \mathbf{Q}_{21}^T) + (\mathbf{A}_{11} - \mathbf{A}_{12} \mathbf{Q}_{22}^{-1} \mathbf{Q}_{21}^T)^T \mathbf{P}_{ismc} - \mathbf{P}_{ismc} \mathbf{A}_{12} \mathbf{Q}_{22}^{-1} \mathbf{A}_{12}^T \mathbf{P}_{ismc} + (\mathbf{Q}_{11} - \mathbf{Q}_{12} \mathbf{Q}_{22}^{-1} \mathbf{Q}_{21}^T) = 0 \quad (69)$$

The optimal  $\mathbf{v}$  minimizing Eq. (67) is as follows,

$$\mathbf{v} = -\mathbf{Q}_{22}^{-1}\mathbf{A}_{12}^T\mathbf{P}_{ismc}\mathbf{z}_1 \quad (70)$$

This expression is substituted into (66)

$$\mathbf{z}_2 = -\mathbf{Q}_{22}^{-1}(\mathbf{A}_{12}^T\mathbf{P}_{ismc} + \mathbf{Q}_{21})\mathbf{z}_1 \quad (71)$$

Comparing Eq. (71) with (55) yields,

$$\mathbf{S}_2^{-1}\mathbf{S}_1 = \mathbf{Q}_{22}^{-1}(\mathbf{A}_{12}^T\mathbf{P}_{ismc} + \mathbf{Q}_{21}) \Rightarrow \mathbf{S}_1 = \mathbf{S}_2\mathbf{Q}_{22}^{-1}(\mathbf{A}_{12}^T\mathbf{P}_{ismc} + \mathbf{Q}_{21}) \quad (72)$$

The non-singular  $\mathbf{S}_2$  is chosen arbitrarily, and then  $\mathbf{S}_1$  is calculated. Finally, matrix  $\mathbf{S} = [\mathbf{S}_1 \ \mathbf{S}_2]$  is created, and the optimal sliding surface is obtained by substituting  $\mathbf{S}$  into Eq. (57).

In summary, all calculation step by step is as follows: First, the orthogonal transformation matrix  $\mathbf{T}$  is determined. The regular form of the system equation (47) is determined by Eq. (49)-(51). The sub-matrices are determined by Eq. (52). The sub-matrices of the transformed matrix  $\mathbf{Q}_{ismc}$  are determined by Eq. (61). The matrix Riccati Eq. (69) concerning  $\mathbf{P}_{ismc}$  is solved. By considering  $\mathbf{S}_2$  as an identity matrix, Eq. (72) is solved, and  $\mathbf{S}$  is obtained. The optimal surface vector  $\sigma$  is determined by Eq. (57). Finally, the positive constants  $k$  and  $\rho$  are chosen large enough, and all findings are substituted into Eq. (59).

### 3. DC SERVO MACHINE MATHEMATICAL MODEL

The linear quadratic algorithms discussed in this paper are all implemented in linear systems. DC servo motor is one of the prevalent devices used to control a system. The performance of the algorithms can be examined by implementing any DC servo motor. Under this heading, the mathematical model of the DC motor is discussed.

DC servo motor consists of two separate partitions. The stator includes field windings. The other partition has armature windings. The right side of Figure 5 presents the armature circuit partition of the DC motor. The other side presents the field circuit partition (Krishnan, 2001; Krause et al., 2002).

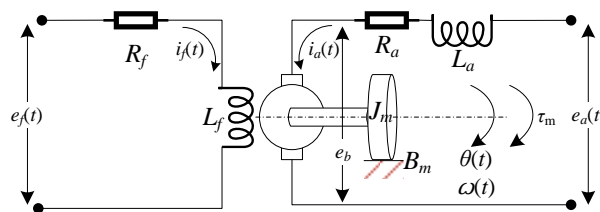


Figure 5. DC servo motor electromechanical diagram

Air gap flux  $\Phi$  is proportional to field current  $i_f$ ,

$$\Phi = K_{fd}i_f \quad (73)$$

where  $K_{fd}$  is the constant between field current,  $i_f$ , and gap flux  $\Phi$ , namely field coil constant. The rotor shaft generates  $\tau_m$  torque, proportional to the product of air gap flux and the armature current.

$$\tau_m(t) = \Phi K_{am}i_a(t) \quad (74)$$

where  $K_{am}$  is the armature coil constant. Substituting (73) into (74) yields

$$\tau_m(t) = K_a i_a(t) \quad (75)$$

where the overall armature constant  $K_a$  is

$$K_a = K_{fd} K_{am} i_f \quad (76)$$

The armature behaves like a generator which produces a back electromotive force  $e_b(t)$  while the armature is rotating. It is also proportional to the shaft angular velocity  $\omega(t)$ .

$$e_b(t) = K_b \frac{d\theta(t)}{dt} = K_b \omega(t) \quad (77)$$

where  $K_b$  is back electromotive force constant. There is a potential difference between the armature windings leads.

$$e_a(t) - e_b(t) = L_a \frac{di_a}{dt} + R_a i_a \quad (78)$$

where  $e_a(t)$  is the applied armature voltage,  $R_a$  is the electrical resistance of the armature circuit,  $i_a$  the armature current, and  $L_a$  is the armature circuit's electrical inductance. Substituting Eq. (77) into (78) and taking the derivative of armature current alone yields

$$\frac{di_a(t)}{dt} = -\frac{K_b}{L_a} \omega(t) - \frac{R_a}{L_a} i_a(t) + \frac{1}{L_a} e_a(t) \quad (79)$$

The rotor partition produces the mechanical movement of the motor. The algebraic sum of all torques,  $\tau$ , equals the product of inertia torque  $J_m$  and angular acceleration  $\alpha$ .

$$\sum \tau = J_m \alpha \quad (80)$$

The total torque consists of electrical torque, friction torque (proportional to angular velocity and opposite to electrical torque), and load torque (opposite in direction). Thus, Eq. (80) is expressed again as,

$$\tau_m - \tau_L - B_m \omega(t) = J_m \alpha \quad (81)$$

where  $\tau_L$  is load torque,  $B_m$  is motor viscous friction constant. Substituting Eq. (75) into Eq. (81) and isolating the angular acceleration alone concludes as follows,

$$\alpha(t) = -\frac{B_m}{J_m} \omega(t) + \frac{K_a}{J_m} i_a(t) - \frac{1}{J_m} \tau_L \quad (82)$$

There is a differential relationship between angular acceleration  $\alpha$ , angular velocity  $\omega$ , and angular position  $\theta$  as follows,

$$\alpha(t) = \frac{d^2}{dt^2} \theta(t), \quad \omega(t) = \frac{d}{dt} \theta(t) \quad (83)$$

The following equation is obtained by substituting Eq. (83) into Eq. (82).

$$\frac{d^2}{dt^2}\theta(t) = \frac{d}{dt}\omega(t) = -\frac{B_m}{J_m}\omega(t) + \frac{K_a}{J_m}i_a(t) - \frac{1}{J_m}\tau_L \quad (84)$$

The state space model can be created by combining Eq. (83), (84), and Eq. (79).

$$\frac{d}{dt} \begin{bmatrix} \theta(t) \\ \omega(t) \\ i_a(t) \end{bmatrix} = \begin{bmatrix} 0 & 1 & 0 \\ 0 & -\frac{B_m}{J_m} & \frac{K_a}{J_m} \\ 0 & -\frac{K_b}{L_a} & -\frac{R_a}{L_a} \end{bmatrix} \begin{bmatrix} \theta(t) \\ \omega(t) \\ i_a(t) \end{bmatrix} + \begin{bmatrix} 0 & 0 \\ -\frac{1}{J_m} & 0 \\ 0 & \frac{1}{L_a} \end{bmatrix} \begin{bmatrix} \tau_L \\ e_a \end{bmatrix} \quad (85)$$

The output equation of the system,

$$\mathbf{y} = [1 \quad 0 \quad 0] \begin{bmatrix} \theta(t) \\ \omega(t) \\ i_a(t) \end{bmatrix} \quad (86)$$

The system matrices are as follows,

$$\mathbf{x} = \begin{bmatrix} \theta(t) \\ \omega(t) \\ i_a(t) \end{bmatrix}, \quad \mathbf{A} = \begin{bmatrix} 0 & 1 & 0 \\ 0 & -\frac{B_m}{J_m} & \frac{K_a}{J_m} \\ 0 & -\frac{K_b}{L_a} & -\frac{R_a}{L_a} \end{bmatrix}, \quad \mathbf{B} = \begin{bmatrix} 0 & 0 \\ -\frac{1}{J_m} & 0 \\ 0 & \frac{1}{L_a} \end{bmatrix}, \quad \mathbf{u} = \begin{bmatrix} \tau_L \\ e_a \end{bmatrix}, \quad \mathbf{C} = [1 \quad 0 \quad 0] \quad (87)$$

The load torque is not an ordinary input; it may be considered a disturbance. Thus, the matrix  $\mathbf{B}$  and vector  $\mathbf{u}$  change as follows.

$$\mathbf{B} = \begin{bmatrix} 0 \\ 0 \\ 1 \\ \frac{1}{L_a} \end{bmatrix}, \quad \mathbf{u} = e_a \quad (88)$$

## 4. COMPUTATIONAL FINDINGS

This section presents numerical results by applying the control strategies discussed in the previous subsections to the DC motor's mathematical model.

### 4.1. Motor Model and Parameter Rates

The DC motor parameter rates, which are used to examine the performance of the LQR-based algorithms in the section above, are as follows:

$$\begin{array}{llll} \text{Voltage supply}=240 \text{ V}, & \text{Rated current}=10 \text{ A}, & B_m=0.002953 \text{ N}\cdot\text{m}\cdot\text{s}, & J_m=0.02215 \text{ kg}\cdot\text{m}^2, \\ K_a=1.011 \text{ N}\cdot\text{m}/\text{A}, & K_b=1.011 \text{ V}/(\text{rad}/\text{s}), & L_a=0.028 \text{ H}, & R_a=2.581 \Omega \end{array}$$

According to the parameter rates above, the DC motor system matrices are as follows,

$$\mathbf{A} = \begin{bmatrix} 0 & 1 & 0 \\ 0 & -0.1333 & 45.6433 \\ 0 & -36.1071 & -92.1786 \end{bmatrix}, \quad \mathbf{B} = \begin{bmatrix} 0 \\ 0 \\ 35.7143 \end{bmatrix}, \quad \mathbf{C} = [1 \quad 0 \quad 0] \quad (89)$$

### 4.2. LQR Controller Calculations

To obtain optimal state feedback gain matrix, using the matrices and vector in Eq. (89), the Eq. (6) and Eq. (14) are calculated respectively. The state and input weight matrices are chosen as  $\mathbf{Q}=\text{diag}([1 \ 1 \ 1])$  and  $\mathbf{R}=1$ . The solutions of Eq. (6) and Eq. (14) are as Eq. (90) and (91), respectively.

$$\mathbf{P}_{lqr} = \begin{bmatrix} 1.4723 & 0.0651 & 0.0280 \\ 0.0651 & 0.0375 & 0.0127 \\ 0.028 & 0.0127 & 0.0109 \end{bmatrix} \quad (90)$$

$$\mathbf{K}_{lqr} = [1 \quad 0.4526 \quad 0.3886] \quad (91)$$

Eq. (91) is substituted into Figure 2, and the linear quadratic state feedback application works. However, the reference desired input vector  $\mathbf{x}_d$  must be calculated by considering the derivative of state variables in Eq. (85) equals zero. In addition, the load torque is deemed a disturbance, so it is considered zero, too.

$$\mathbf{x}_d = \begin{bmatrix} \theta_d \\ 0 \\ 0 \end{bmatrix} \quad (92)$$

$\theta_d$  is the desired angular position.

### 4.3. LQR With Integral Control Calculations

The optimal linear quadratic gain matrix is obtained by making extended matrices in Eq. (23) and solving Eq. (26)-(27), respectively. The state and input weight matrices are decided upon as  $\mathbf{Q}_{lqri} = \text{diag}([1 \ 1 \ 1 \ 1])$  and  $\mathbf{R}=1$ . The extended matrices are as follows,

$$\mathbf{A}_{lqri} = \begin{bmatrix} 0 & 1 & 0 & 0 \\ 0 & -0.13 & 45.65 & 0 \\ 0 & -36.1071 & -92.1786 & 0 \\ -1 & 0 & 0 & 0 \end{bmatrix}, \quad \mathbf{B}_{lqri} = \begin{bmatrix} 0 \\ 0 \\ 35.7143 \\ 0 \end{bmatrix} \quad (93)$$

The solutions of Eq. (26) and Eq. (27) are as follows.

$$\mathbf{P}_{lqri} = \begin{bmatrix} 2.9797 & 0.1309 & 0.0562 & -1.5164 \\ 0.1309 & 0.0404 & 0.0139 & -0.0655 \\ 0.0562 & 0.0139 & 0.0114 & -0.0280 \\ -1.5164 & -0.0655 & -0.0280 & 2.0082 \end{bmatrix} \quad (94)$$

$$\mathbf{K}_x = [2.0082 \quad 0.4967 \quad 0.4075], \quad \mathbf{K}_{in} = -1 \quad (95)$$

$\mathbf{K}_{in}$  and  $\mathbf{K}_x$  are substituted into Figure 3, and LQR with integral action can be realized.

### 4.4. Optimal PID Controller Calculations

The designing PID controller consists of calculating the controller parameters so that the system behaves as desired. The desired behavior may require an optimized control input or settling time optimization. This subsection proposes designing an optimal PID controller equivalent to an optimal state feedback controller. The optimal PID controller algorithm works based on the sequential calculation of equations Eq. (42)-(45). The state and input weight matrices are selected to serve as  $\bar{\mathbf{Q}} = \text{diag}([1 \ 1 \ 1 \ 1])$  and  $\mathbf{R}=1$ . The output of the algorithm allows the optimal PID controller to gain matrices. According to the system matrices (89), the algorithm's output gives the controller gains as  $\mathbf{K}_p=2.0082$ ,  $\mathbf{K}_i=1$ , and  $\mathbf{K}_d=0.4967$ . This output is substituted into the block diagram in Figure 4, and the optimal PID algorithm works.

### 4.5 Optimal Sliding Mode

The whole solution algorithm is discussed in the final paragraph in section 0. The state and input weight matrices are utilized due to their purpose as  $\mathbf{Q}_{ismc} = \text{diag}([1 \ 1 \ 1 \ 1 \ 1])$  and  $\mathbf{R}=1$ . According to the suggested solution, all calculations give the following results:

$$\mathbf{P}_{ismc} = \begin{bmatrix} 2 & 803 & 0 & 803 & -112 \\ 803 & -5277 & 0 & -5170 & -36650 \\ 0 & 0 & 0 & 0 & 0 \\ 803 & -517 & 0 & -5063 & -36665 \\ -112 & -3.665 & 0 & -3.6665 & 5106 \end{bmatrix} \cdot 10^4 \quad (96)$$

$$\mathbf{S} = [-1.0407 \quad 2.0217 \quad -1 \quad 0 \quad 0 \quad 0] \quad (97)$$

$$\boldsymbol{\sigma} = [-2.0217 \quad -1.0407 \quad -1 \quad -1 \quad 0 \quad 0] \quad (98)$$

Eq. (98) is substituted into Eq. (59), and the control signal is applied to the system.  $k$  and  $\rho$  constants should be selected large enough. They are selected as 50 and 5, respectively.

## 5. SIMULATION RESULTS

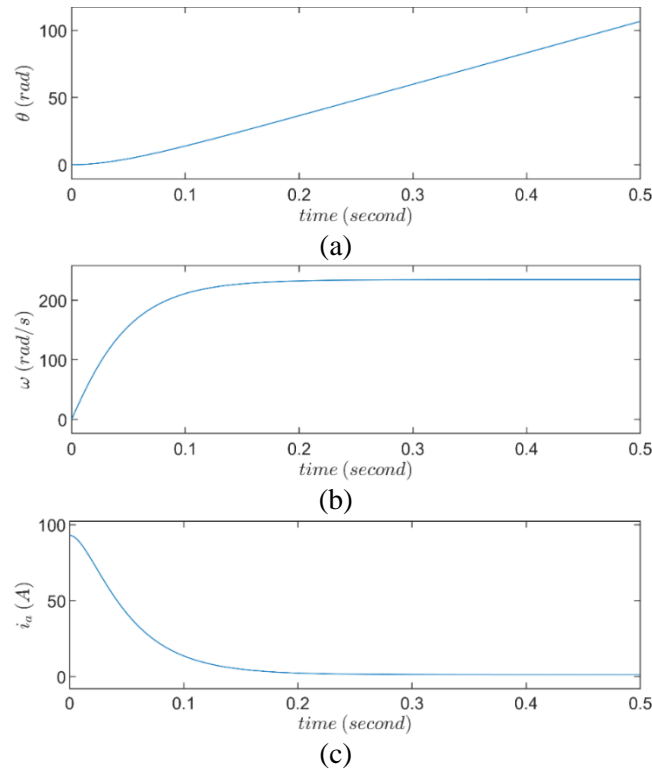
The illustrative results are related to the optimal control algorithms presented in previous sections.

Figure 6 demonstrates the step response of the DC motor for which the parameters are presented in Section 0. The armature voltage is chosen as 240 V as the step function input. The field windings are supplied with 300 V to provide magnetization. The field current is measured as 1.0665 A. Figure 6a shows the angular replacement of the DC motor shaft. It also seems it does not have a settling time of angular position. Figure 6b illustrates that the angular speed of the DC motor reaches the stable speed of 234.3 rad/s in 0.2 seconds.

The system appears unstable when the DC motor is considered a system with armature voltage as the input and angular position as the output. It is also insensitive to disturbances and load torque. Elimination of the lack of robustness, the controllers are required to be used.

Figure 7 demonstrates the simulation result of the whole DC motor control system. The reference angular speed is chosen as  $\theta_r = \pi/2$  radian and applied to the control system as a step function beginning at the end of the first second. Figure 7a shows that the optimal PID controller and ISMC respond with overshoot. However, the other controllers have responses without overshoot. All angular position responses settle in about five seconds. The load torque equals zero at the beginning. As seen in Figure 7e, the load torque is applied to the system as a disturbance input  $T_L = 0.5$  Nm at the 15<sup>th</sup> second—all optimal control algorithms respond to the load torque disturbance input except the LQR. The optimal control algorithms' robustness is caused by the integral term used in LQRI, PID, and ISMC. LQR seems to have no robustness against load disturbance, resulting in a collapsing position control response after 15 seconds. However, the other controllers have robust responses, so their responses settle in about six seconds with no steady-state error. Figure 7b depicts the angular velocity derivative of the angular position. It reaches zero speed within six seconds. Figure 7c shows the armature current, which has a settling time of less than three seconds. Figure 7d illustrates the system signal's control signal. It seems the most reactive behavior belongs to the ISMC. It has the chattering phenomena by its nature. Once the load torque is applied to the system, all algorithms exhibit nearly identical behaviors except the LQR.

The variations in the values of cost functions within the first 15 seconds are shown in Figure 8. The cost function associated with the PID controller exhibits a notably faster increase than the others. Over time, the cost function that increases at the slowest rate is attributed to the LQR controller.



**Figure 6.** DC motor step response of the state variables when the  $e_a=240$  V and  $e_f=300$  V. **a)** angular position **b)** angular speed **c)** armature current

## 6. CONCLUSIONS

The study explicates some optimal control techniques and depicts their performances by implementing the DC motor for position control. LQR-based control does not perform as robustly as other controllers. When the load torque is applied as a disturbance, the ISMC behaves robustly for angular position control. A single LQR-based controller does not seem as robust and sufficient as it can eliminate the disturbance-based error. However, LQR with an integral action controller eliminates the error. Besides, the other control algorithms seem to possess similar robustness.

This study's comparative analysis is crucial in selecting the robust and optimal controller. The LQR control includes the least number of terms, but it does not have enough robustness. LQRI action contains an extra state variable term compared to the single LQR. The optimal PID controller needs to have an extra one-state variable. The ISMC contains a state variable two times more than the original system, but the robustness seems acceptable.

The DC motor model, which has three state variables, is used for examining the algorithms. LQR and ISMC controllers need all system state variables to be measurable or observable. However, the optimal PID controller needs only output to be measurable. This situation necessitates obtaining all state variables through estimation when LQR and SMC-based algorithms are employed. This study considers all DC motor state variables measurable or observable. At the same time, LQR and SMC-based algorithms are employed.

The optimal algorithms are designed for a linear system. Employing the optimal algorithms with observers for nonlinear systems and time-delayed systems can be a future work. Luenberger filter or Kalman filter are well-known observers for obtaining the unmeasurable state variables of any system. Using optimal control algorithms with observers will provide more detailed information about their usability.

In applications requiring time optimization, the power applied to the system input does not need to be limited. Optimal control will be helpful, especially in systems requiring energy saving and power and mechanical energy applications.

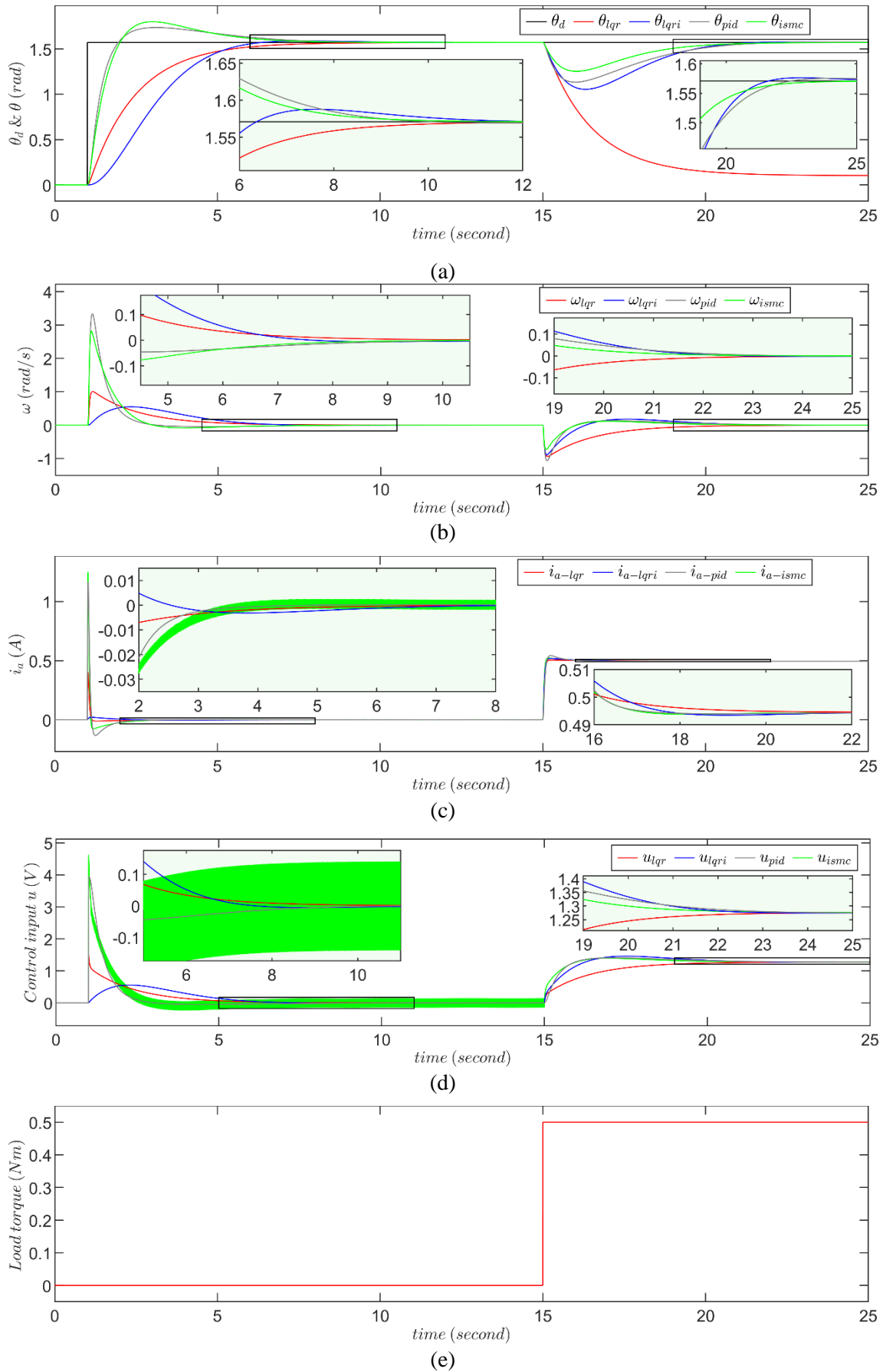


**Figure 7.** The step response simulation results in DC motor control system **a)** angular position **b)** angular speed **c)** armature current **d)** control input signal **e)** load torque

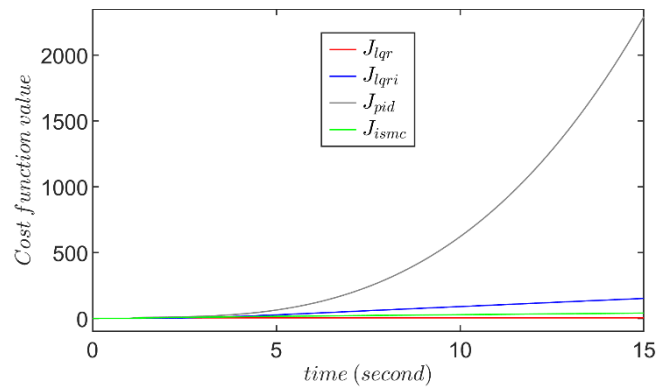


**Figure 8.** The values of the cost functions according to time

## CONFLICT OF INTEREST

The author declares no conflict of interest.

## REFERENCES

- Anderson, B. D., & Moore, J. B. (2007). *Optimal Control Linear Quadratic Methods* (91.12 edition ed.). Dover Publications.
- Aravind, M. A., Saikumar, N., & Dinesh, N. S. (2017, May 19-21). *Optimal position control of a DC motor using LQG with EKF*. In: Proceedings of the International Conference on Mechanical, System and Control Engineering (ICMSC), (pp. 149-154). St. Petersburg. <https://www.doi.org/10.1109/ICMSC.2017.7959461>
- Burns, R. S. (2001). *Advanced Control Engineering*. Woburn, England: Butterworth-Heinemann.
- Davis, J. H. (2002). Luenberger Observers. In: *Foundations of Deterministic and Stochastic Control* (pp. 245-254). Boston: Birkhäuser. [https://www.doi.org/10.1007/978-1-4612-0071-0\\_8](https://www.doi.org/10.1007/978-1-4612-0071-0_8)
- Dorf, R. C., & Bishop, R. H. (2010). *Modern Control Systems* (12th ed.). (M. J. Horton, A. Gilfillan, A. Dworkin, S. Disanno, G. Dulles, & D. Sandin, Eds.) New Jersey, U.S.A.: Pearson.
- Dreyfus, S. (1962). Variational problems with inequality constraints. *Journal of Mathematical Analysis and Applications*, 4(2), 297-308. [https://doi.org/10.1016/0022-247X\(62\)90056-2](https://doi.org/10.1016/0022-247X(62)90056-2)
- Durdu, A., & Dursun, E. H. (2019). Sliding Mode Control for Position Tracking of Servo System with a Variable Loaded DC Motor. *Elektronika Ir Elektrotechnika*, 25(4), 8-16. <https://www.doi.org/10.5755/j01.eie.25.4.23964>
- Edwards, C., & Spurgeon, S. K. (1998). *Sliding Mode Control Theory and Applications*. Boca Raton: CRC Press.
- Eli, S. C., Idoniboyeobu, D. C., & Braide, S. L. (2023). Performance Evaluation of D.C. Motor Speed Using Sliding Mode Controller (SMC). *Journal of Emerging Trends in Electrical Engineering*, 5(3), 1-6.
- Feng, X., Liu, S., Yuan, Q., Xiao, J., & Zhao, D. (2023). Research on wheel-legged robot based on LQR and ADRC. *Scientific Reports*, 13(15122). <https://www.doi.org/10.1038/s41598-023-41462-1>
- Franklin, G. F., Powell, J. D., & Emami-Naeini, A. (2009). *Feedback Control of Dynamic Systems* (6th ed.). New Jersey, U.S.A.: Pearson Education.
- Gao, W., & Hung, J. C. (1993). Variable Structure Control of Nonlinear Systems A New Approach. *IEEE Transactions On Industrial Electronics*, 40(1), 45-55.
- Golub, G. H., & Loan, C. F. (2013). *Matrix Computations*. Baltimore: The Johns Hopkins University Press.
- Gorczyca, P., Hajduk, K., & Kołek, K. (2011). Optimal Control of A Laboratory DC Servo Motor. *Pomiary automatyka Robotyka*, 15(12), 129-134.

- He, S., Duan, X., Qu, X., & Xiao, J. (2023). Kinematic modeling and motion control of a parallel robotic antenna pedestal. *Robotica*, 41(11), 3275-3295. <https://www.doi.org/10.1017/S0263574723000917>
- Jouini, M., Dhahri, S., & Sellami, A. (2019). Combination of integral sliding mode control design with optimal feedback control for nonlinear uncertain systems. *Transactions of the Institute of Measurement and Control*, 41(5), 1331-1339. <https://www.doi.org/10.1177/0142331218777562>
- Khomenko, M., Voytenko, V., & Vagapov, Y. (2013). Neural Network based Optimal Control of Dc Motor Positioning System. *International Journal of Automation and Control*, 7(1/2), 83-104. <https://www.doi.org/10.1504/IJAAC.2013.055097>
- Kirk, D. E. (1998). *Optimal Control Theory: An Introduction*. New York, Mineola, USA: Dover Publications, Inc.
- Krause, P. C., Wasynczuk, O., & Sudhoff, S. D. (2002). *Analysis of Electric Machinery and Drive Systems* (2nd ed.). U.S.A.: John Wiley & Sons.
- Krishnan, R. (2001). *Electric Motor Drives Modeling Analysis and Control* (1st ed.). New Jersey: Prentice Hall.
- Maghfiroh, H., Anwar, M., Anwar, M., & Ma'arif, A. (2022). Improved LQR Control Using PSO Optimization and Kalman Filter Estimator. *IEEE Access*, 10, 18330-18337. <https://www.doi.org/10.1109/ACCESS.2022.3149951>
- Mamta, & Singh, B. (2020). Optimal Control of DC motor using Equilibrium Optimization Algorithm. *International Journal of Engineering Research & Technology (IJERT)*, 9(5), 1272-1275.
- Mondal, R., & Dey, J. (2020). Performance Analysis and Implementation of Fractional Order 2-DOF Control on Cart-Inverted Pendulum System. *IEEE Transactions On Industry Applications*, 56(6), 7055-7066.
- Mukhopadhyay, S. (1978). P.I.D. Equivalent of Optimal Regulator. *Elektronics Letters*, 14(25), 821-822.
- Naidu, D. S. (2002). *Optimal Control Systems* (1st ed.). CRC Press.
- Nise, N. S. (2011). *Control System Engineering* (6th ed.). Pomona, U.S.A.: John Wiley & Sons, Inc.
- Ogata, K. (2010). *Modern Control Engineering* (5th ed.). Natick: Pearson.
- Paraskevopoulos, P. N. (2002). *Modern Control Engineering*. CRC Press.
- Pontryagin, L. S. (1986). *The Mathematical Theory of Optimal Processes* (Vol. Vol 4). Switzerland: Gordon and Breach Science Publishers.
- Pratama, G. N., Setiawan, N., Saputra, S. A., Pambudi, L., Umam, A. D., & Hermansah, M. N. (2022). Optimal Quadratic Regulator PID for Motor DC. *Journal of Physics: Conference Series*, 2406(012002), 1-7. <https://www.doi.org/10.1088/1742-6596/2406/1/012002>
- Rasheed, L. T. (2020). Optimal Tuning of Linear Quadratic Regulator Controller Using Ant Colony Optimization Algorithm for Position Control of a Permanent Magnet Dc Motor. *Iraqi Journal of Computers, Communications, Control & Systems Engineering (IJCCCE)*, 20(3), 29-41. <https://www.doi.org/10.33103/uot.ijccce.20.3.3>
- Ruderman, M., Krettek, J., Hoffmann, F., & Bertram, T. (2008). Optimal State Space Control of DC Motor. *IFAC Proceedings Volumes*, 41(2), 5796-5801. <https://www.doi.org/10.3182/20080706-5-KR-1001.00977>
- Saputra, D. D., Ma'arif, A., Maghfiroh, H., Baballe, M. A., Tusset, A. M., Sharkawy, A.-N., & Majdoubi, R. (2023). Performance Evaluation of Sliding Mode Control (SMC) for DC Motor Speed Control. *Jurnal Ilmiah Teknik Elektro Komputer dan Informatika (JITEKI)*, 9(2), 502-510.
- Simon, D. (2006). *Optimal State Estimation*. Hoboken: John Wiley & Sons.
- Tanveer, A., & Ahmad, S. M. (2023). Design and Testing Of a Compact Inexpensive Prototype Remotely Operated Underwater Vehicle for Shallow Water Operation. *Journal of Naval Architecture and Marine Engineering*, 20(1), 1-10.

- Utkin, V. I. (1977). Variable Structure Systems with Sliding Modes. *IEEE Transactions On Automatic Control*, 22(2), 212-222. <https://www.doi.org/10.1109/TAC.1977.1101446>
- Utkin, V. I. (1992). *Sliding mode In Control and Optimization*. New York, U.S.A.: Springer.
- Utkin, V. I. (1993). Sliding Mode Control Design Principles and Applications to Electric Drives. *IEEE Transactions On Industrial Electronics*, 40(1), 23-36. <https://www.doi.org/10.1109/41.184818>
- Utkin, V. I., & Parnakh, A. (1978). *Sliding Modes and their Application in Variable Structure Systems* (Russian) (1st ed.). Mir.
- Utkin, V. I., & Yang, K. D. (1978). Methods for construction of discontinuity planes in multidimensional variable structure systems. *Automat. i Telemekh.*, (10), 72-77.
- Utkin, V. I., Guldner, J., & Shi, J. (2009). *Sliding Mode Control in Electromechanical Systems* (2nd ed.). CRC Press.
- Wang, B., Liu, C., Chen, S., Dong, S., & Hu, J. (2019). Data-Driven Digital Direct Position Servo Control by Neural Network With Implicit Optimal Control Law Learned From Discrete Optimal Position Tracking Data. *IEEE Access*, 7, 126962-126972. <https://www.doi.org/10.1109/ACCESS.2019.2937993>
- Xiang, Z., & Wei, W. (2021). Design of DC motor position tracking system based on LQR. *Journal of Physics: Conference Series*, 1887, 012052. <https://www.doi.org/10.1088/1742-6596/1887/1/012052>
- Yousef, A. M. (2011). Experimental Set up Verification of Servo Dc Motor Position Control Based On Integral Sliding Mode Control Approach. *Journal of Engineering Sciences*, 39(5), 1095-1110.
- Yu, G.-R., Tseng, M.-H., & Lin, Y.-K. (2004, September 2-4). *Optimal Positioning Control of a DC Servo Motor Using Sliding Mode*. In: Proceedings of the 2004 IEEE International Conference on Control Applications. Taipei. <https://www.doi.org/10.1109/CCA.2004.1387223>